BUTTERWORTH HEINEMANN

Polymer Vol. 36 No. 7, pp. 1435–1440, 1995

0032-3861/95/$10.00 + 0.00

Small penetrant diffusion in polybutadiene: a molecular dynamics simulation study

Richard H. Gee and Richard H. Boyd*
Departments of Materials Science and Engineering, Chemistry and Chemical Engineering, University of Utah, Salt Lake City, UT 84112, USA
(Received 19 July 1994; revised 14 September 1994)

Molecular dynamics (MD) simulations have been used to study the diffusion of methane as a small molecule penetrant example in *cis*-1,4-polybutadiene (PBD). The non-bonded potential for an 'anisotropic' united atom (AUA) representation of the –CH= group was calibrated by adjusting the constants to fit experimental volume temperature data for the polymer melt. This potential was used along with an already available AUA function for the $-CH_2-$ group. The diffusion coefficient of methane was determined via MD simulation over a wide range of temperature. The results agree well with near room temperature experimental values for N_2 in *cis*-PBD. The latter gas is similar in diffusion behaviour to methane. The mechanism of diffusion in terms of the nature of the diffusive jump process and its response to temperature is found to be similar to that in atactic polypropylene and polyethylene melts. At low temperatures the penetrant is trapped for relatively long periods in a cage of surrounding polymer and makes occasional large jumps. As temperature increases the size of the jumps increases further. The quiescent trapped periods disappear and a liquid-like scattering regime prevails. This change in mechanism as temperature increases is accompanied by a decrease in activation energy. The diffusion in PBD is faster than in other hydrocarbon polymers studied so far by simulation (polyethylene, polyisobutylene and atactic polypropylene). The order of diffusion coefficients correlates with the free volumes available in the polymer hosts.

(Keywords: diffusion; molecular dynamics simulation; *cis*-1,4-polybutadiene)

INTRODUCTION

The diffusion of penetrants through polymers is a subject of longstanding interest from both a practical and fundamental point of view. Polymers are often employed for their barrier properties. In order to understand the factors governing permeability it is desirable to have a molecular-level understanding of the mechanism of diffusion. Further, it would be very desirable to be able to make predictions about the likely barrier characteristics of polymers from the chemical structure of the repeat units. Molecular dynamics (MD) simulations are a promising tool for achieving these goals[1–6]. In this method the time trajectories of all the constituent atoms, including the permeants, are followed in detail by integrating the classical equations of motion. Diffusion coefficients are inferred from the random walk nature of the penetrant motion. The method is computationally intensive but with present-day computer capabilities it is now practical.

Elastomers have been an important class of polymers in the context of diffusion and many experimental studies concerning them have been carried out[7]. In the present work, diffusion in a typical elastomer is studied via MD simulation. The polymer system chosen is *cis*-1,4-polybutadiene (*cis*-PBD). It has relative structural simplicity and experimental data exist concerning both its physical properties and the diffusion of penetrants in it. To be consistent with our previous studies[4–6] methane is chosen as the penetrant. Methane is the largest of the simple gas permeants commonly studied experimentally and conforms well to representation as a single-centre united atom (UA) CH_4 group.

Since penetrant diffusion is highly sensitive to free volume in the host it is very important that the polymer matrix be realistically modelled in the simulations. Especially important is the capability of the simulations to represent correctly the volume *versus* temperature characteristics of the host. Thus part of the work reported here is devoted to achieving this capability. This takes the form of ensuring that the non-bonded potentials that determine the packing characteristics are properly calibrated. Volume–temperature (V–T) data for *cis*-PBD are used to calibrate a new 'anisotropic' united atom (AUA) potential[8] for the =CH– group. The AUA potential is a function only of the distance between interacting centres. However, it has the feature of the force centres being displaced from the carbon atom of the group toward the hydrogen of the C–H bond. We also use a previously developed AUA potential for the $-CH_2-$ group[9].

COMPUTATIONAL DETAILS

The polymer system studied consisted of a single polymer chain of *cis*-PBD. The chain contained 768 united atom (UA) centres, or, $[-CH_2-CH=CH-CH_2-]_{192}$. Cubic periodic boundary conditions were invoked. The initial

* To whom correspondence should be addressed

PBD configurations were generated at 450 K for isolated chains, after which the periodic boundary conditions were imposed. A very large initial periodic box was allowed to shrink to the appropriate volume, using the constant particle number, pressure, and temperature (NPT) method of Nosé[10]. The volume shrinking process was allowed to equilibrate to constant average volume. The total equilibration time utilized was 500 ps. Following this step, the systems were cooled in NPT runs to the various temperatures studied in steps of 50 K for 200–500 ps each. The pressure was set to zero, which is indistinguishable from 1 atm. The cooling rate and rate of volume equilibration are largely determined by the thermal and inertial mass parameters in the Nosé method. These were selected to be given fairly rapid equilibration but fluctuations in temperature and volume that are acceptable. The inertial mass parameters selected ranged from 5×10^2 (atm s^2 m^{-3}) at the lowest temperature to 1×10^4 (atm s^2 m^{-3}) at the highest. The thermal mass parameter ranged from 10^{-15} J s^2 at low temperature to 10^{-14} J s^2 at high.

All intramolecular degrees of freedom were considered, but the bond stretching constants were reduced by a factor of 4 compared with spectroscopic values to allow an increase in the time step in the numerical integration of the equations of motions. A value of 1 fs was used for the latter. The NPT dynamic equations of motion were solved using a five-term Gear predictor–corrector algorithm[11].

The potential function constants for bond bending, stretching and torsion are listed in *Table 1*. They are the same as values recently selected in a study of conformational dynamics in PBD[12]. The sources of the constants are detailed there. However, in the present work a new =CH– group AUA potential was developed in order to have a good representation of the V–T properties of the polymer. The ε well-depth and σ distance of crossing zero energy along with the AUA offset distance, d, were adjusted to give agreement between the MD-generated V–T curve and the experimental one and also to give agreement with estimates of the cohesive energy density (see below for the agreement attained).

Table 1 Potential functions[a]

Function	Constants	
C–C bond stretch energy = $1/2k_R(R-R_0)^2$		
$-CH_2-CH_2-$	$k_R = 663$	$R_0 = 1.54$
$=CH-CH_2-$	$k_R = 769$	$R_0 = 1.50$
$-CH=CH-$	$k_R = 1033$	$R_0 = 1.335$
Bond bending energy = $1/2k_\theta(\theta-\theta_0)^2$		
$-CH_2-$	$k_\theta = 482$	$\theta_0 = 111.6$
$=CH-$	$k_\theta = 374$	$\theta_0 = 124.0$
Torsional potential about $-CH_2-CH_2-$		
$1/2V_3(1+\cos 3\phi)+1/2V_1(1+\cos\phi)$	$V_3 = 13.4$	$V_1 = 3.35$
Torsional potential about $-CH_2-CH=$		
$1/2V_3(1-\cos 3\phi)$	$V_3 = 7.95$	
Torsional potential about $-CH=CH-$		
$1/2V_2(1-\cos 2\phi)$	$V_2 = 58.6$	
AUA non-bonded potential, Lennard-Jones 6–12[b]		
$-CH_2-$	$\varepsilon = 0.686$	$R_{min} = 3.94$
	$\sigma = 3.510$	$d = 0.42$
$=CH-$	$\varepsilon = 0.50$	$R_{min} = 3.70$
	$\sigma = 3.30$	$d = 0.08$
CH_4	$\varepsilon = 1.18$	$R_{min} = 4.27$
	$\sigma = 3.80$	$d = 0.0$

[a] Energies in kJ mol^{-1}, distances in Å, angles in radians (shown above in degrees). The potentials are from ref. 12 with the exception of the =CH– group non-bonded function developed here and the methane function which is from ref. 5

[b] For the $-CH_2-$ and =CH– group the potential is of the AUA (anisotropic united atom) type, the interaction centre is offset from the C atom by the distance d along the bisector of the C–C–C angle in the direction of the hydrogens; ε is the well-depth; R_{min} the distance at the minimum; σ is the distance at the energy zero

The studies of polymer–penetrant diffusion were carried out under constant volume, temperature and particle number (NVT) conditions. The NVT conditions were accomplished using the Nosé NPT method but the values of the intertial parameter were chosen to be large enough to ensure that the volume remained constant. At higher temperatures (350–450 K) a single penetrant was used, thereby avoiding any possible cross-correlation effects. However, at lower temperatures (250–325 K) it was necessary to use four methane penetrants to enhance the statistics associated with the diffusion trajectories and thus obtain reliable predictions of the diffusion coefficients. In the multiple-diffusant systems, it was ensured that no two penetrant molecules were less than 10 Å apart at the time of insertion. In addition, the slow diffusive nature of the penetrant under low temperatures precluded the coordinated motion of two or more penetrants on the time-scale of the MD runs. The diffusion coefficients were determined from the slopes of $\langle R_p^2 \rangle$ *versus* t curves as

$$D = \langle R_p^2 \rangle / 6t \qquad (1)$$

where R_p is the distance that the penetrant traverses over the time t. The averaging implied by the angled brackets is accomplished by regarding numerous points along the time trajectory as the starting point of a new trajectory. The time interval, Δt, between successive origins is ideally chosen such that no correlation exists between the penetrant motion at time t and later at time $t+\Delta t$ and the penetrant will have undergone many fluctuations in Δt. In practice, Δt was chosen to be 1 ps, thus ensuring that no diffusive information in the penetrant trajectory was lost since Δt is much shorter than that of the positional autocorrelation decay. The runs are long enough to be certain that the linear region in $\langle R_p^2 \rangle$ *versus* t is observed. Any initial cage effect and long-time noise due to disappearance of multiple trajectories in the averaging are discounted.

The PBD polymer–penetrant systems were studied at seven temperatures: 450, 400, 375, 350, 325, 300 and 250 K. At each temperature, the polymer–penetrant systems were allowed to reach equilibrium over MD runs of 500 ps, after which penetrant diffusion trajectories were accumulated. The lengths of the diffusion runs from which slopes of the mean-square penetrant displacement, $\langle R_p^2 \rangle$, *versus* time were extracted ranged from 500 to 1000 ps. The lengths of the runs were determined by the time required for the clear emergence of the long-time linear region in $\langle R_p^2 \rangle$ *versus* time curve. *Figure 1* displays a resultant $\langle R_p^2 \rangle$ curve for methane in *cis*-PBD at 250 K using four penetrants and *Figure 2* displays results at 400 K for a single penetrant. Several distinguishing characteristics are displayed in *Figures 1* and *2*. First, the non-linear region at very short times (the offset from zero) is due to the fast ballistic motion of the penetrant between polymer–penetrant collisions. Second, at intermediate times, the cage effect region of the curve, the motion of the penetrant is still found to be correlated and not yet diffusive. Third, the long-time region represents the truly

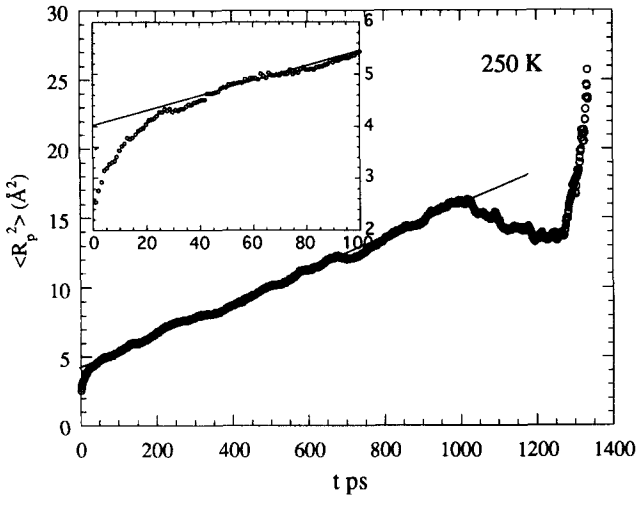

Figure 1 Mean-squared displacement *versus* time for methane diffusing in *cis*-PBD at 250 K. The data are obtained from the trajectories of four penetrants. The inset is a blow-up of the early time region

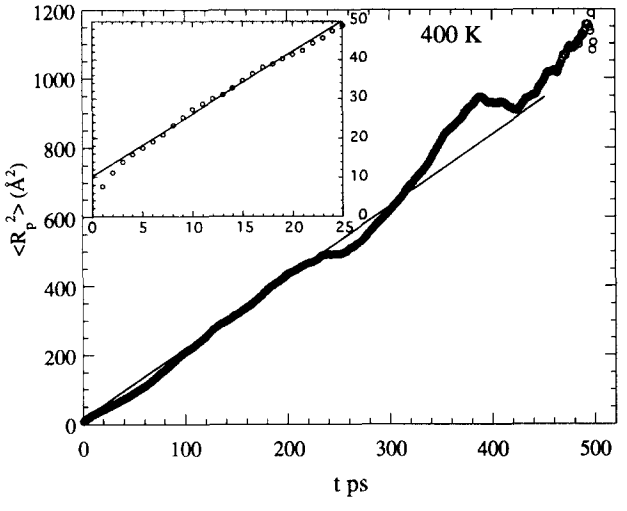

Figure 2 Mean-squared displacement *versus* time for methane diffusing in *cis*-PBD at 400 K. The data are obtained from the trajectory of a single penetrant. The inset is a blow-up of the early time region

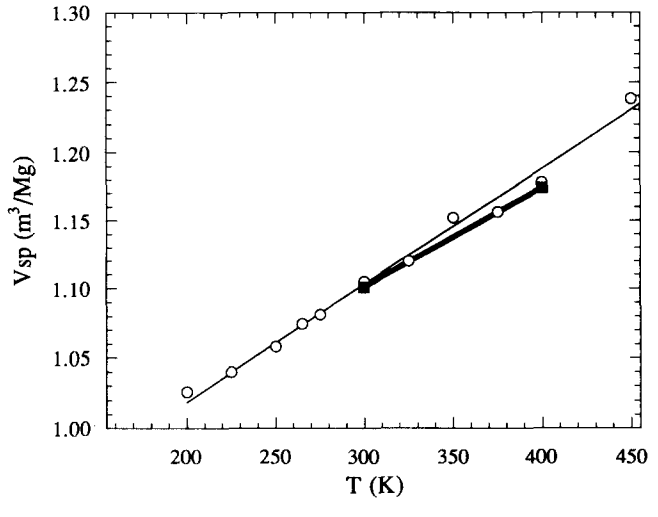

Figure 3 Specific volume of *cis*-PBD *versus* temperature. The open circles smoothed by the fine line are from NPT MD simulation. The heavy line anchored by filled squares is from experimental data, ref. 13

diffusive or statistical nature of the diffusion process, it is in this region that $\langle R_p^2 \rangle$ is linear with time. Fourth, at very long times, on the order of the total MD run length, the total number of subtrajectories over which averaging is performed is much less and the curves become erratic.

RESULTS AND DISCUSSION

Volume versus *temperature and cohesive energy results*

The volume *versus* temperature at zero pressure points for *cis*-PBD determined from the NPT MD runs are shown in *Figure 3*. They are compared with the experimental data of DiBenedetto and Paul[13]. It is apparent from *Figure 3* that the agreement is reasonably good. The coefficient of thermal volume expansion, α_T, is $7.7 \times 10^{-4}\,K^{-1}$ from the MD points and $6.6 \times 10^{-4}\,K^{-1}$ from experiment.

The cohesive energy density is calculated from the intermolecular non-bonded energy and the system volume. For a description of the separation of inter *versus* intra nonbonded energy for single chain MD systems, see ref. 9. The square root of this is the solubility parameter. A value of the latter at 300 K of $16.4\,MPa^{1/2}$ is obtained. This compares to literature values[14] in the range $16.6–17.6\,MPa^{1/2}$.

Characteristic ratio

Another quantity from the MD simulation that can be compared with experiment is the characteristic ratio. This is defined as $C_N = \langle R^2 \rangle / Nl^2$ where $\langle R^2 \rangle$ is the average end-to-end distance, N is the number of bonds and l is the bond length. In the case here for PBD where there are three kinds of bonds this is generalized to

$$C_N = \langle R^2 \rangle \Big/ \sum_{i=1}^{3} N_i l_i^2 \qquad (2)$$

where $\langle R^2 \rangle$ is the average end-to-end distance, N_i is the number of bonds of each bond type (i.e. CH_2–CH_2, CH_2–CH and CH=CH) and l_i is the corresponding bond length.

Values of C_∞, the value of the characteristic ratio in the high molecular weight limit, are available from experiment. In the MD simulations direct observation of R^2 for the end-to-end distance of the entire chain of 192 monomers is not possible for several reasons. First of all, the statistics of the averaging would be very poor because the equilibration time would be very long. Second, the periodic boundary conditions introduce artifacts. Interatomic distances between groups farther apart than one-half of the periodic box size ($\sim 30/2$ Å $= \sim 15$ Å) are subject to these effects. However, values of $\langle R_{ij}^2 \rangle$ where R_{ij} is the distance between chain groups i and j can be computed. Then C_N can be extrapolated *versus* $N = |j - i|$. Actually, since C_N asymptotically approaches C_∞ the extrapolation is better made against $1/N$. *Figure 4* shows such a plot for *cis*-PBD at 300 K. An artifactual turndown in the curve at small $1/N$ may be seen. Thus it is apparent that an asymptotic slope at small $1/N$ is not precisely established. However, it also appears that a meaningful estimate of C_N can be made. The intercept at $1/N = 0$ gives a value of $C_N = 4.2$. Two experimental values for 100% *cis*-PBD from intrinsic viscosity measurements in theta solvents are 4.9 and 5.1[15]. Values for predominantly *cis* polymer that contains 2–4% 1,2-configurations are in

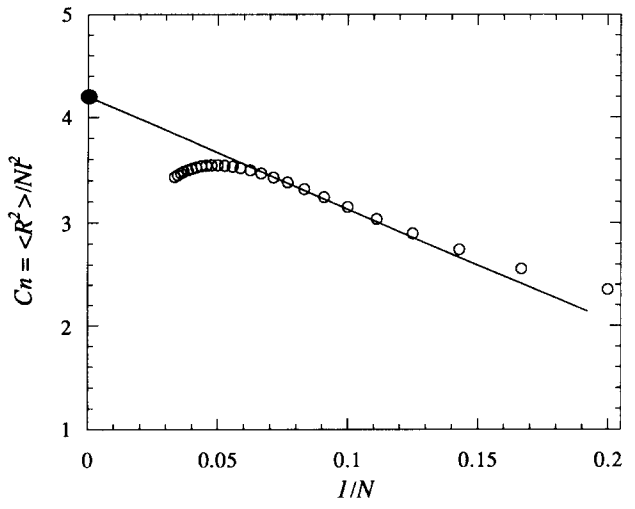

Figure 4 The high molecular weight limiting characteristic ratio (●) of *cis*-PBD at 300 K as determined by extrapolation of $\langle R^2\rangle/Nl^2$ *versus* $1/N$ (○); $\langle R^2\rangle$ is the mean-square distance between beads separated by N bonds of length l

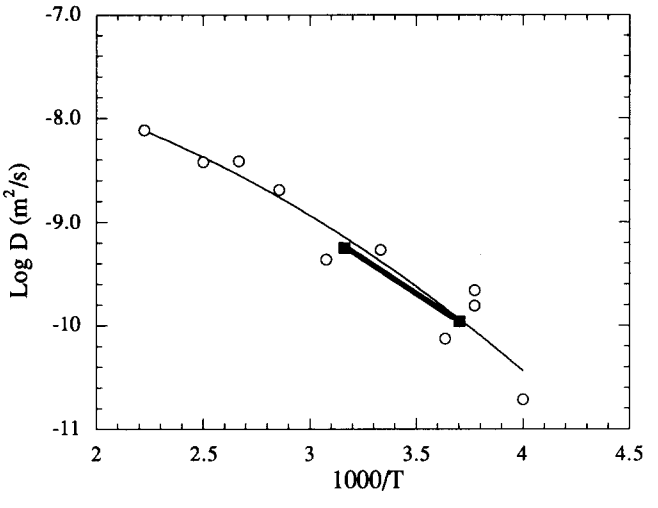

Figure 5 Arrhenius plot of the diffusion coefficient for methane in *cis*-PBD from MD simulation (○). The fine curve is a smoothing second-order polynomial. Experimental results for nitrogen diffusing in *cis*-PBD are shown as the heavy line anchored by filled squares, ref. 13

the range 4.2 to 4.8[15]. Thus it would seem that the MD value is probably a bit low but in reasonable agreement with experiment. The effect of steric interactions in *cis*-PBD on the characteristic ratio from the point of view of the rotational isomeric state model has been investigated in detail by Mark[16]. Interferences involving the $-CH_2-$ groups when the $-CH_2-C=$ bonds are in the *cis* conformation were predicted to reduce the populations of these conformations. This has the effect of making the characteristic ratio larger than it otherwise would be. We find this effect in our MD studies as well[12].

Comparison of penetrant diffusion coefficients with experiment

The MD-determined diffusion coefficients calculated here for methane in *cis*-PBD are plotted in *Figure 5* as $\log D$ *versus* $1/T$. Also shown are experimental results for nitrogen in the same polymer[13]. Methane diffuses at about 60–80% of the rate for nitrogen in a number of polymers[17]. Thus the difference in $\log D$ for the two gases should be minor. On this basis it may be concluded that the simulations give diffusion coefficients in agreement with experiment.

Diffusion mechanism

Viewed in total detail (femtosecond scale) the penetrant trajectory is dominated by segments of straight-line ballistic motion separated by collisions with the neighbouring polymer beads. Many of these collisions only result in the penetrant visiting a closed region or cage formed by the surrounding beads. Some of the collisions result in the penetrant establishing a new environment and true diffusive motion results. In the multiple origin averaging process the ballistic region has upward curvature in the $\langle R_p^2\rangle$ *versus* t plot. On the time-scale of a plot useful for diffusion coefficient determination this region appears only as an intercept at $t=0$. The cage effect is observed in the plot as an asymptotic approach with negative curvature to the straight-line portion. These effects are illustrated in *Figures 1* and 2.

It is of interest to investigate in more detail the nature of the diffusive jumps. In order to separate the latter from the cage effect motions a filtering process is required. This is conveniently accomplished by the following procedure[5]. The average position of the diffusant is computed over a specified time interval. This position is compared with that of the succeeding interval and a jump distance computed. The time interval is selected to be long enough that the short-time cage effect is filtered out but short enough that the diffusive jumps remain. The latter can be verified by comparing the filtered trajectory with the unfiltered one to see that the same diffusion coefficient is obtained.

The above procedure was followed in computing temporal history or jump sequence maps for methane diffusing in *cis*-PBD. The results at 250 and 450 K are shown in *Figure 6*. At low temperature (250 K) the jumps are well separated in time. Occasionally the diffusant makes a fairly large jump. This is consistent with the

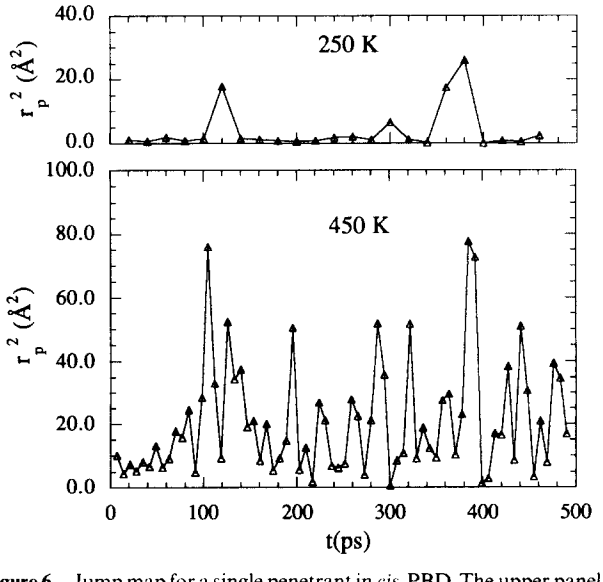

Figure 6 Jump map for a single penetrant in *cis*-PBD. The upper panel is at 250 K, the lower one is at 450 K. The squared displacement, r_p^2, is computed between successive 20 ps positional averages of the penetrant at 300 K; at 400 K the interval is 7 ps

penetrant moving by a mechanism in which the matrix appears fairly solid-like and hops are made to new sites. At a higher temperature (450 K) the jumps are so frequent as to be poorly resolved in time. Also the average jump size is larger than at low temperature. This is consistent with the matrix appearing more mobile and the diffusant progress is a more liquid-like scattering process with the cage playing less of a role. It may be seen by comparing the inserts in *Figures 1* and *2* that the lifetime of the cage is much shorter at the higher temperature. It may be seen in *Figure 5* that a decrease in activation energy accompanies the transition from the hopping regime to the liquid-like region.

The decreasing activation energy effect is found in simulations of diffusion in other polymers. *Figure 7* shows a comparison of the $\log D$ *versus* $1/T$ behaviour for polyethylene (PE)[5], polyisobutylene (PIB)[5] and atactic polypropylene (aPP)[6] with the present results for *cis*-PBD. In PE and aPP it was found that a similar change in diffusion mechanism takes place with temperature. It may be seen in *Figure 7* that the activation energy also decreases with increasing temperature in these polymers.

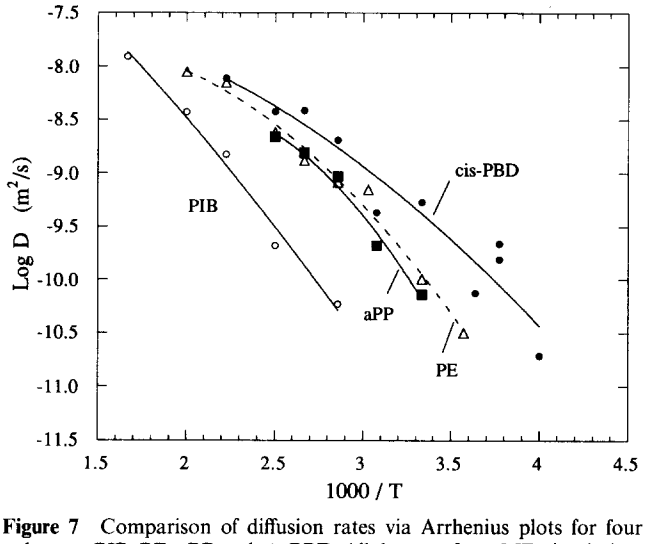

Figure 7 Comparison of diffusion rates via Arrhenius plots for four polymers; PIB, PE, aPP and *cis*-PBD. All data are from MD simulation, the data for PIB, PE and aPP are from previous work[5,6]. The curves are smoothing second-order polynomials

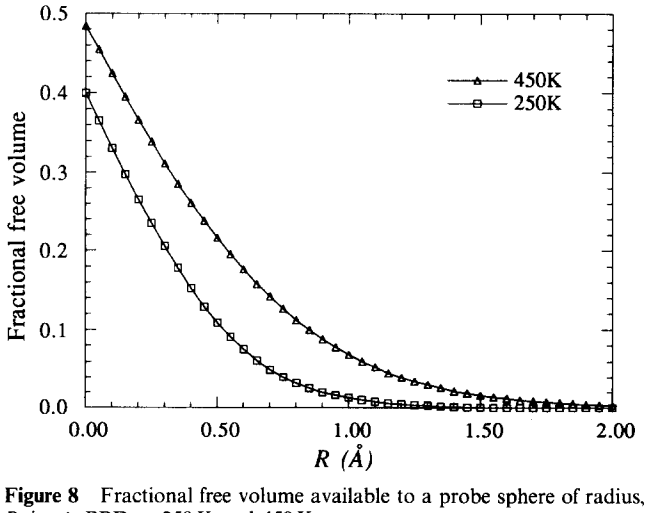

Figure 8 Fractional free volume available to a probe sphere of radius, R, in *cis*-PBD at 250 K and 450 K

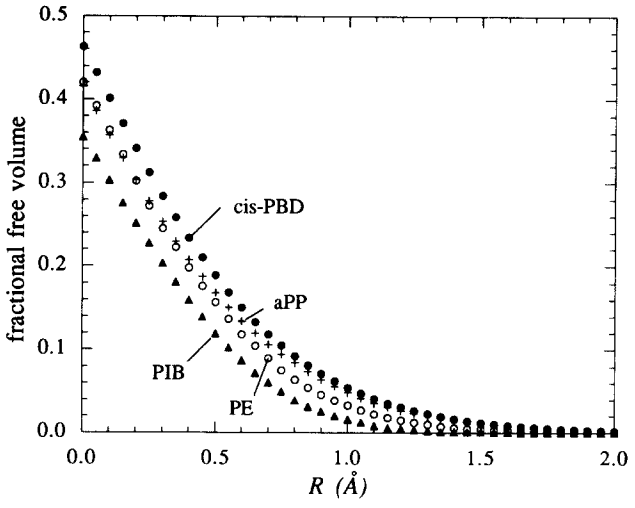

Figure 9 Fractional free volume available to a probe sphere of radius, R, compared for PIB, PE, aPP and *cis*-PBD at 400 K

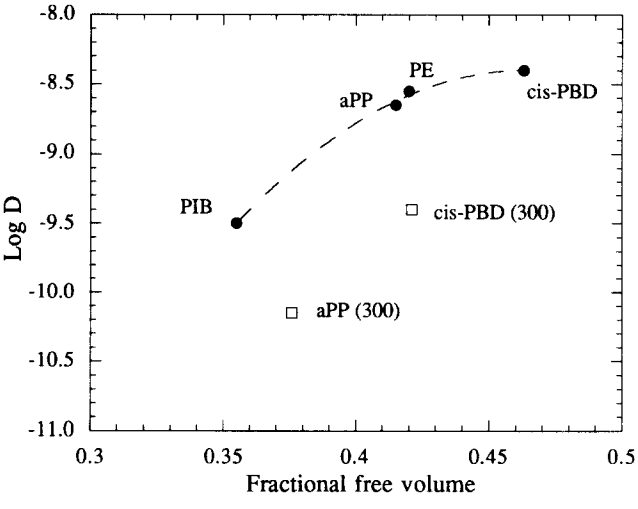

Figure 10 Correlation of diffusion rate with free volume. Log of the diffusion coefficient (*Figure 7*) *versus* fractional free volume both at 400 K (●---●). For aPP and *cis*-PBD points (□) are also shown at 300 K

In PIB, where the diffusion is much slower, the mechanism remains in the solid-like hopping regime over the temperature range studied[5]. The decrease in activation energy with increasing temperature has been observed experimentally in the diffusion of methane in PE[5] and also for the diffusion of benzene in nature rubber, *cis*-polyisoprene[18].

Diffusion and free volume

It is apparent in *Figure 7* that there are considerable differences in the penetrant diffusion rates between the polymers considered. Diffusion in PIB is much slower than in the others. The rates in PE and aPP are similar. The diffusion in *cis*-PBD is significantly faster than in the others. It is of interest to be able to correlate these observations with the structure and packing in the hosts. A densely and efficiently packed matrix should result in slow diffusion in comparison with a loosely packed one. A much invoked simple measure of these effects is the

free volume. In order to test the usefulness of this concept we have computed the free volume in *cis*-PBD. Measures are already available for the other polymers previously studied by simulation[6]. The free volume used here and previously is based on the volume not occupied by spheres of Lennard-Jones diameter, σ (see *Table 1*) for the $-CH_2-$ and $=CH-$ UA groups. *Figure 8* displays the fractional free volume available to a probe sphere of radius, R, for *cis*-PB at 450 and 250 K. In *Figure 9* comparison is made with the other polymers studied so far. It may be seen in *Figure 9* that the order of free volumes is the same as the order of diffusion rates in *Figure 7*. PIB has a significantly lower free volume and diffusion rate than the others, the rates and free volumes in PE and aPP are similar and the free volume and diffusion rate in *cis*-PBD are higher than in the others. This is more transparently displayed in *Figure 10* where $\log D$ at 400 K is plotted against the total fractional free volume (i.e. for probe sphere radius = 0) at the same temperature. It is apparent that a smooth correlation exists. However, it also appears that free volume *per se* is not a sufficient descriptor. Points plotted for aPP and *cis*-PBD at 300 K show that an iso-free volume condition, independent of temperature, does not describe diffusion rates.

ACKNOWLEDGEMENTS

The authors are indebted to the Exxon Chemical Company for support of their work. They are also grateful to the Utah Supercomputing Institute, where many of the computations were done, for the use of their facilities.

REFERENCES

1 Trohalaki, S., Kloczkowski, A., Mark, J. E., Rigby, D. and Roe, R. J. in 'Computer Simulation of Polymers' (ed. R. J. Roe), Prentice Hall, New York, 1991, pp. 220
2 Sok, R. M., Berendsen, J. C. and van Gunsteren, W. F. *J. Chem. Phys.* 1992, **96**, 4699
3 Mueller-Plathe, F. *J. Chem. Phys.* 1992, **96**, 3200
4 Pant, P. V. K. and Boyd, R. H. *Macromolecules* 1992, **25**, 494
5 Pant, P. V. K. and Boyd, R. H. *Macromolecules* 1993, **26**, 679
6 Han, J. and Boyd, R. H. *Macromolecules* 1994, **27**, 5365
7 Crank, J. and Park, G. S. (eds) 'Diffusion in Polymers' Academic Press, New York, 1968
8 Toxvaerd, S. *J. Chem. Phys.* 1990, **93**, 4290
9 Pant, P. V. K., Han, J., Smith, G. D. and Boyd, R. H. *J. Chem. Phys.* 1993, **99**, 597
10 Nosé, S. *J. Chem. Phys.* 1984, **81**, 511
11 Allen, M. P. and Tildesley, D. J. 'Computer Simulation of Liquids', Clarendon Press, Oxford, 1987
12 Gee, R. H. and Boyd, R. H. *J. Chem. Phys.* 1994, **101**, 8028
13 Paul, D. R. and Di Benedetto, A. T. *J. Polym. Sci. C* 1965, **10**, 17
14 Grulke, E. A. in 'Polymer Handbook', 3rd edn (Eds J. Brandrup and E. H. Immergut), Wiley-Interscience, New York, 1989
15 Kurata, M. and Tsunashima, Y. in 'Polymer Handbook', 3rd edn (Eds J. Brandrup and E. H. Immergut), Wiley-Interscience, New York, 1989, p. VII 1
16 Mark, J. E. *J. Am. Chem. Soc.* 1966, **88**, 4354
17 Stannett, V. in 'Diffusion in Polymers' (Eds J. Crank and G. S. Park), Academic Press, New York, 1968, Ch. 2
18 Fujita, H. in 'Diffusion in Polymers' (Eds J. Crank and G. S. Park), Academic Press, New York, 1968, Ch. 3